

Cholesterol-lowering drugs cause dissolution of cholesterol crystals and disperse Kupffer cell crown-like structures during resolution of NASH

George N. Ioannou,^{1,*} Derrick M. Van Rooyen,[†] Christopher Savard,^{*} W. Geoffrey Haigh,^{*} Matthew M. Yeh,[§] Narci C. Teoh,[†] and Geoffrey C. Farrell[†]

Division of Gastroenterology, Department of Medicine,^{*} Veterans Affairs Puget Sound Health Care System and University of Washington, Seattle, WA; Liver Research Group,[†] Australian National University Medical School at the Canberra Hospital, Garran, ACT, Australia; and [§]Department of Pathology, University of Washington, Seattle, WA

Abstract Cholesterol crystals form within hepatocyte lipid droplets in human and experimental nonalcoholic steatohepatitis (NASH) and are the focus of crown-like structures (CLSs) of activated Kupffer cells (KCs). Obese, diabetic *Alms1* mutant (*foz/foz*) mice were fed high-fat (23%) diet containing 0.2% cholesterol for 16 weeks and then assigned to four intervention groups for 8 weeks: a) vehicle control, b) ezetimibe (5 mg/kg/day), c) atorvastatin (20 mg/kg/day), or d) ezetimibe and atorvastatin. Livers of vehicle-treated mice developed fibrosing NASH with abundant cholesterol crystallization within lipid droplets calculated to extend over 3.3% (SD, 2.2%) of liver surface area. Hepatocyte lipid droplets with prominent cholesterol crystallization were surrounded by TNF α -positive (activated) KCs forming CLSs (≥ 3 per high-power field). KCs that formed CLSs stained positive for NLRP3, implicating activation of the NLRP3 inflammasome in response to cholesterol crystals. In contrast, *foz/foz* mice treated with ezetimibe and atorvastatin showed near-complete resolution of cholesterol crystals [0.01% (SD, 0.02%) of surface area] and CLSs (0 per high-power field), with amelioration of fibrotic NASH. Ezetimibe or atorvastatin alone had intermediate effects on cholesterol crystallization, CLSs, and NASH. These findings are consistent with a causative link between exposure of hepatocytes and KCs to cholesterol crystals and with the development of NASH possibly mediated by NLRP3 activation.—Ioannou, G. N., D. M. Van Rooyen, C. Savard, W. G. Haigh, M. M. Yeh, N. C. Teoh, and G. C. Farrell. Cholesterol-lowering drugs cause dissolution of cholesterol crystals and disperse Kupffer cell crown-like structures during resolution of NASH. *J. Lipid Res.* 2015. 56: 277–285.

Supplementary key words crown-like structure • caspase 1 • lipotoxicity • nonalcoholic steatohepatitis

Nonalcoholic fatty liver disease (NAFLD) is characterized by increased lipid deposition within hepatocytes attributable to metabolic causes in the absence of viral hepatitis or liver disorders caused by excessive alcohol or toxic drug consumption or other liver disorders. In the majority of patients, NAFLD manifests histologically as “simple steatosis” defined as hepatic steatosis without substantial inflammation or fibrosis. Simple steatosis carries a very low risk of progression to cirrhosis and liver dysfunction (1). However, 10–30% of patients with NAFLD have or develop nonalcoholic steatohepatitis (NASH), characterized by hepatic lobular inflammation and fibrosis in addition to steatosis. Progression to cirrhosis occurs in a proportion of patients (1, 2).

The factor(s) responsible for the development of progressive NASH, as opposed to simple steatosis, remain unclear. A prominent concept that has been invoked to explain the development of NASH is that of lipotoxicity. Hepatic lipotoxicity implies that exposure to, or accumulation of, certain lipid species within hepatic cells may directly cause cellular toxicity or act in a proinflammatory or profibrotic manner. According to the hypothesis of hepatic lipotoxicity, NASH develops when the liver is exposed to lipotoxic lipid species, whereas simple steatosis develops in response to over-nutrition when the liver is not significantly exposed to lipotoxic lipid species. It is generally accepted that triglycerides, which constitute the majority of hepatic lipids in NASH and simple steatosis, are a “safe” storage lipid with little or no lipotoxic potential. Relatively small quantities of other lipotoxic lipid species may exert a disproportionate impact in the development of NASH.

Lipidomic analyses of human livers with NAFLD reported that levels of free (unesterified) cholesterol (FC) were increased in NASH but not in simple steatosis, whereas levels of

This work was supported by a grant from the Diabetes Research Center, University of Washington (G.N.I.) and by resources from VAPSHCS Research and Development.

Manuscript received 8 August 2014 and in revised form 8 December 2014.

Published, JLR Papers in Press, December 17, 2014

DOI 10.1194/jlr.M053785

Abbreviations: Ath, atherogenic; CLS, crown-like structure; FC, free cholesterol; IL, interleukin; KC, Kupffer cell; NAFLD, nonalcoholic fatty liver disease; NASH, nonalcoholic steatohepatitis.

¹To whom correspondence should be addressed.

e-mail: georgei@medicine.washington.edu

free fatty acids were no different (3). Recent experimental studies suggest that FC is an important lipotoxic molecule that promotes the development of NASH (3–12). Thus, using diverse animal models [dietary with cholesterol-containing atherogenic (Ath) diets (4, 5, 7), LDLR knock-out and ApoE knock-in mice (9–12), appetite-defective *Alms1* mutant (*foz/foz*) (6, 8), or melanocortin 4 receptor-deficient (*Mc4r-ko*) (13) mice fed an Ath diet, and *ABCB4* mutant opossums with defective hepatic cholesterol excretion in bile (14)], there is support for a consistent association between hepatic FC content and NASH pathology. Human epidemiological studies and nonrandomized clinical trials of cholesterol-lowering drugs also appear to support a role of cholesterol in the development of NASH (15–17).

The mechanisms by which cholesterol, a naturally occurring molecule abundant in most tissues, might exert lipotoxicity and promote the development of NASH remain unclear. We recently reported that cholesterol crystals were present within the lipid droplets of steatotic hepatocytes in patients with NASH and in a mouse model of NASH induced by a high-fat, high-cholesterol diet but not in patients or mice with simple steatosis (18). We also demonstrated that enlarged Kupffer cells (KCs) surrounded steatotic, dead hepatocytes containing cholesterol crystals. Such KCs appeared to process the remnant lipid droplets within these hepatocytes to form characteristic crown-like structures (CLSs) similar to those recently described in inflamed visceral adipose tissue (19, 20). This lipid scavenging resulted in profound accumulation of cholesterol within small droplets in markedly enlarged, activated KCs that took the appearance of the lipid-laden “foam cells” found in atheroma. These findings are particularly relevant because cholesterol crystals have recently been shown to activate the NLRP3 inflammasome in animal models of atherosclerosis (21, 22), thus providing a mechanism by which exposure of KCs to cholesterol crystals could lead to chronic inflammation and resultant fibrosis in NASH.

In the current study, we used a combination of approaches to test this concept. We explored a metabolic syndrome murine model of NASH [*Alms1* mutant (*foz/foz*) mice], in which an appetite defect leads to obesity, diabetes, and metabolic syndrome (as in *Mc4r-ko* mice), to determine whether *a*) the links between hepatic cholesterol crystals, CLSs, and NASH are reproducible in a completely different animal model from the one used initially to describe these findings and *b*) pharmacological treatment aimed at reducing hepatic cholesterol content also removed hepatic cholesterol crystals, leading to resolution of crown-like structures in association with reversal of NASH fibrosis.

METHODS

Animal procedures

These experiments were performed on mice used previously to analyze the therapeutic effects of cholesterol-lowering drugs on NASH pathology (8). In brief, female *Alms1* mutant (*foz/foz*) mice were fed a high-fat (23%), high-sucrose diet containing 0.2% cholesterol (Specialty Feeds, Australia), hereafter referred

to as an Ath diet, for 16 weeks, then assigned to one of four pharmacological groups for an additional 8 weeks while continuing the Ath diet. Agents were administered orally with the diet as previously reported (8): *a*) vehicle control ($n = 8$); *b*) atorvastatin ($n = 10$), 20 mg/kg body weight/day (Lipitor®; Pfizer West Ryde, NSW, Australia); *c*) ezetimibe ($n = 10$), 5 mg/kg/day (Ezetrol®; Schering-Plough, Whitehouse Station, NJ); and *d*) ezetimibe, 5 mg/kg/day and atorvastatin, 20 mg/kg/day ($n = 9$).

The *foz/foz* mice have a spontaneous mutation of the Alström syndrome gene murine equivalent, *Alms1*, which is associated with loss of hypothalamic neuronal cilia causing severely defective central appetite regulation (23). This results in hyperphagia, rapid weight gain with inactivity, obesity, insulin resistance, hypercholesterolemia, and NAFLD. We previously reported that in *foz/foz* mice intake of an Ath diet accelerates the development of obesity, insulin resistance, hyperinsulinemia, hyperglycemia, hypercholesterolemia, hypodiponectinemia, hypertension (metabolic syndrome), and transformation of simple steatosis to NASH (6). Thus, *foz/foz* mice on the Ath diet mirror the metabolic and histological features of human NASH. Similar findings have been noted in mice with other hypothalamic appetite defects, such as *Mc4r-ko* mice (13), reflecting the importance of *Alms1* as an appetite disorder with no direct implications for liver biology (hepatocytes do not express a primary cilium).

Experiments were approved by the Australian National University Experimentation Ethics Committee (Canberra, Australia) and by the Research and Development Committee of the Veterans Affairs Puget Sound Health Care System (Seattle, WA).

Hepatic histological assessment

Formalin-fixed, paraffin-embedded liver sections were stained with hematoxylin and eosin and Sirius red (for collagen). Histological steatosis, inflammation, ballooning degeneration, and fibrosis were assessed semiquantitatively by a “blinded” liver pathologist to determine the NAFLD Activity Score and the overall impression of NASH according to the scoring system proposed by Kleiner et al. (24).

Assessment of hepatic cholesterol crystals and FC

Frozen mouse liver tissue embedded in Optimal Cutting Temperature compound was sectioned at 10 μm in thickness. Sections were allowed to come to room temperature and were immediately cover-slipped using pure glycerol as the mounting medium without applying stain. They were examined using a Nikon Eclipse microscope with or without a polarizing filter to evaluate for the presence of birefringent crystals that we have previously shown to represent cholesterol crystals (18). With the polarizing filter in place, images of 10 random fields were taken (200 \times original magnification; 0.26 mm^2 total area/image) in each liver, avoiding major blood vessels. Image J density software (National Institutes of Health, Bethesda, MD) was used to calculate the percent area of each image that was birefringent, and the average of 10 images per liver was calculated. Frozen liver sections were also stained with filipin to visualize FC (18). Filipin interacts with the 3β -hydroxy group of cholesterol to fluoresce blue (25).

When attempting to demonstrate cholesterol crystals and simultaneously stain for KCs or for FC, the procedures used for these stains (i.e., long incubation times and repeated washing) cause partial disruption of the cholesterol crystals and somewhat diminished birefringence so that they may not appear as prominent as when they are looked at in unprocessed, frozen liver sections.

Assessment of KC crown-like structures and activation of the NLRP3 inflammasome

Frozen liver sections were stained with anti-CD68 and anti-F4/80 antibodies, which identify macrophages (including hepatic

KCs) and with anti-TNF- α antibodies, which identify activated M1 macrophages, as described previously (8, 18). These stains were used to identify activated macrophages surrounding and processing steatotic hepatocytes containing cholesterol crystals to form CLSs. CLSs were counted in 10 random fields (200 \times original magnification) per liver. The percent area that stained with anti-TNF α in 10 random fields per liver was averaged as an assessment of the number of activated macrophages.

We also stained liver sections with anti-CD3e (Life Technologies, Grand Island, NY) and with antimyeloperoxidase (Thermo Scientific, Fremont, CA) to evaluate for involvement of T-cells or neutrophils, respectively, in CLSs.

Liver sections were stained with anti-NLRP3 antibodies (R&D Systems, Minneapolis, MN) to look for expression of this component of the NLRP3 inflammasome in the KCs of CLSs. Liver sections were also stained for activated (cleaved) caspase 1 using the FAM-FLICA caspase 1 assay kit (Immunochemistry Technologies, Bloomington, MN). Detection of cleaved caspase 1 demonstrates the presence of an activated NLRP3 inflammasome: cleaved caspase-1 can mediate the downstream effects of the NLRP3 inflammasome by cleaving and activating pro-interleukin (IL)-1 and pro-IL-18. All primary antibodies were identified using secondary antibodies labeled with AlexaFluor 488 (Invitrogen, Camarillo, CA) examined with the FITC filters on a Nikon fluorescent microscope.

We used real-time PCR to quantify mRNA gene expression levels as previously described (8) of the following components of the NLRP3 inflammasome in liver tissue: *Caspase-1*, *Nalp3*, and *Asc* (apoptosis-associated speck-like, caspase recruitment domain containing protein) (26).

Statistical analyses

Continuous data are presented as mean (\pm SD) and analyzed by ANOVA with Tukey post hoc testing. Histological assessments were done using Kruskal-Wallis test and group comparisons with Mann-Whitney U test. A *P* value <0.05 was considered statistically significant.

RESULTS

Treatment of obese, diabetic mice with ezetimibe and atorvastatin to lower hepatic FC levels resolves hepatocyte cholesterol crystals in association with resolution of NASH

As previously reported (6, 8), Ath-fed *foz/foz* mice develop fibrotic NASH after 24 weeks in association with obesity, hyperinsulinemia, hyperglycemia, hypo adiponectinemia, and increased hepatic FC content (Table 1). Administration of

TABLE 1. Characteristics (mean \pm SD) of *foz/foz* mice after 24 weeks on a high-fat diet with 0.2% cholesterol, categorized by receipt of pharmacological treatment during the last 8 weeks of the experiment

Pharmacological Treatment	Vehicle n = 8	Atorvastatin n = 10	Ezetimibe n = 10	Ezetimibe + Atorvastatin n = 9
Body weight (g)	52.2 \pm 2.3	49.1 \pm 1.6	50.0 \pm 3.3	52.4 \pm 1.4
Liver weight/body weight (%)	10.9 \pm 0.5	8.4 \pm 0.4 ^a	7.3 \pm 0.5 ^a	6.7 \pm 0.4 ^a
Hepatic lipids (mg/g)				
Triglyceride	379 \pm 48	238 \pm 39	283 \pm 40	161 \pm 28 ^a
Cholesterol ester	39.2 \pm 4	15 \pm 4 ^a	11 \pm 3 ^a	4 \pm 2 ^a
Cholesterol	1.3 \pm 0.5	0.7 \pm 0.2	0.7 \pm 0.3	0.4 \pm 0.1 ^a
Serum levels, fasting				
ALT (U/l)	358 \pm 27	206 \pm 20 ^a	151 \pm 41 ^a	88 \pm 19 ^a
Cholesterol (mmol/l)	5.4 \pm 0.4	4.2 \pm 0.3	3.3 \pm 0.4	3.2 \pm 0.4 ^a
HDL cholesterol (mmol/l)	2.2 \pm 0.1	1.8 \pm 0.1	1.6 \pm 0.1 ^a	1.5 \pm 0.2 ^a
Triglyceride (mmol/l)	1.17 \pm 0.1	0.84 \pm 0.1	1.22 \pm 0.19	1.46 \pm 0.3
Glucose (mmol/l)	8.35 \pm 0.3	9.26 \pm 0.7	9.46 \pm 0.5	7.93 \pm 0.2
Insulin (ng/ml)	7.80 \pm 2.2	2.29 \pm 1.09 ^a	3.20 \pm 1.13 ^a	2.62 \pm 0.3 ^a
Adiponectin (ng/ml)	3.38 \pm 0.2	5.9 \pm 0.5 ^a	6.1 \pm 0.7 ^a	7.3 \pm 0.5 ^a
MCP-1 (pg/ml)	193 \pm 23	117 \pm 9 ^a	122 \pm 17 ^a	111 \pm 8 ^a
Hepatic protein expression (relative expression)				
NF- κ B p65 (nuclear)	1.6 \pm 0.1	1.5 \pm 0.1	1.2 \pm 0.0 ^a	1.0 \pm 0.0 ^a
I κ B α (cytoplasmic)	0.9 \pm 0.0	1.3 \pm 0.1	1.5 \pm 0.1 ^a	2.0 \pm 0.2 ^a
VCAM-1 (total)	1.6 \pm 0.1	1.3 \pm 0.1	1.3 \pm 0.1	0.9 \pm 0.0 ^a
ICAM-1 (total)	2.4 \pm 0.1	1.8 \pm 0.1 ^a	2.0 \pm 0.1	1.8 \pm 0.1 ^a
Hepatic histology				
Steatosis (0–3)	2.6 \pm 0.2	2.2 \pm 0.3	2.2 \pm 0.2	1.8 \pm 0.3
Inflammation (0–3)	1.6 \pm 0.2	1.3 \pm 0.3	0.9 \pm 0.2 ^a	0.3 \pm 0.2 ^a
Ballooning (0–2)	2.0 \pm 0.0	1.6 \pm 0.3	1.8 \pm 0.1 ^a	1.8 \pm 0.2 ^a
NAS (0–8)	6.3 \pm 0.2	5.1 \pm 0.6	4.9 \pm 0.3 ^a	4.0 \pm 0.3 ^a
NASH present	100% (8/8)	80% (8/10)	70% (7/10)	22% (2/9) ^a
Fibrosis stage \geq 1	100% (8/8)	90% (9/10)	50% (6/10) ^a	33% (3/9) ^a
Sirius Red staining area	1.03 \pm 0.03	0.42 \pm 0.04 ^a	0.42 \pm 0.20 ^a	0.35 \pm 0.04 ^a
Cytokeratin-18 fragmentation (M30) (% of liver area)	12.0 \pm 1.5	8.4 \pm 1.3	5.3 \pm 1.0 ^a	4.3 \pm 0.9 ^a
Cholesterol crystals area (% of liver area)	3.3 \pm 2.2%	1.0 \pm 1.7%	0.1 \pm 0.1% ^a	0.01 \pm 0.02% ^a
Crown-like structures ^b (number per high-power field)	\geq 3	1–2	0–1 ^a	0 ^a
TNF α staining area (% of liver area)	1.21 \pm 0.5	0.75 \pm 0.3	0.57 \pm 0.3 ^a	0.06 \pm 0.03 ^a

ALT, alanine aminotransferase; ICAM-1, intercellular adhesion molecule 1; MCP-1, monocyte chemoattractant protein-1; NAS, Nonalcoholic Fatty Liver Disease Activity Score; NASH, nonalcoholic steatohepatitis; NF- κ B, nuclear factor kappa B; VCAM-1, vascular cell adhesion molecule 1. Some of the data presented in this table were presented in a different format in a previous publication (8).

^a *P* < 0.05 compared with vehicle-treated mice.

^b Representative examples of the distribution of crown-like structures in each group are shown in Fig. 3.

atorvastatin or ezetimibe, and particularly combined treatment with both, agents lowered hepatic FC content in Ath-fed *foz/foz* mice (Table 1). This was associated with amelioration of NASH, which was present in 22% of mice treated with both ezetimibe and atorvastatin, as compared with 100% of vehicle-treated controls, and with fibrosis (fibrosis stage ≥ 1 present in 33% of mice treated with both ezetimibe and atorvastatin mice as compared with 100% of vehicle-treated controls). Administration of ezetimibe and atorvastatin also resulted in a significant reduction in hepatic histological inflammation scores, hepatic levels of the proinflammatory transcription factor NF- κ B, and its downstream proinflammatory markers vascular cell adhesion molecule 1 and ICAM-1, whereas hepatic expression of the NF- κ B inhibitor B- α (I κ B α) increased (Table 1).

Frozen liver sections of the vehicle-treated *foz/foz* mice exhibited striking birefringence under polarized light within hepatocyte lipid droplets (Fig. 1). Filipin staining confirmed that the birefringent material consisted of cholesterol crystals (Fig. 2). Some lipid droplets were entirely birefringent, appearing as “Maltese crosses,” and the

remaining had specks of birefringence in the periphery of the lipid droplet. The *foz/foz* mice that were treated with both ezetimibe and atorvastatin for the last 8 weeks of the experiment had almost complete resolution of filipin staining and of cholesterol crystals (Fig. 2), which accounted for 0.01% (SD, 0.02) of liver surface area as compared with 3.3% (SD, 2.2) in the vehicle-treated mice ($P < 0.05$) (Table 1). Intermediate levels of cholesterol crystallization were observed in mice treated with atorvastatin alone (1%), and even lower levels (0.1%) of cholesterol crystallization were observed with ezetimibe treatment alone.

Treatment with ezetimibe and atorvastatin caused resolution of hepatic CLSs

Vehicle-treated *foz/foz* mice fed a high-fat diet developed CLSs of activated macrophages identified by TNF α staining surrounding hepatocytes that exhibited intense cholesterol crystallization within large lipid droplets (Fig. 3A, B). CLSs were completely absent in mice treated with ezetimibe and atorvastatin (Fig. 3G, H). In mice

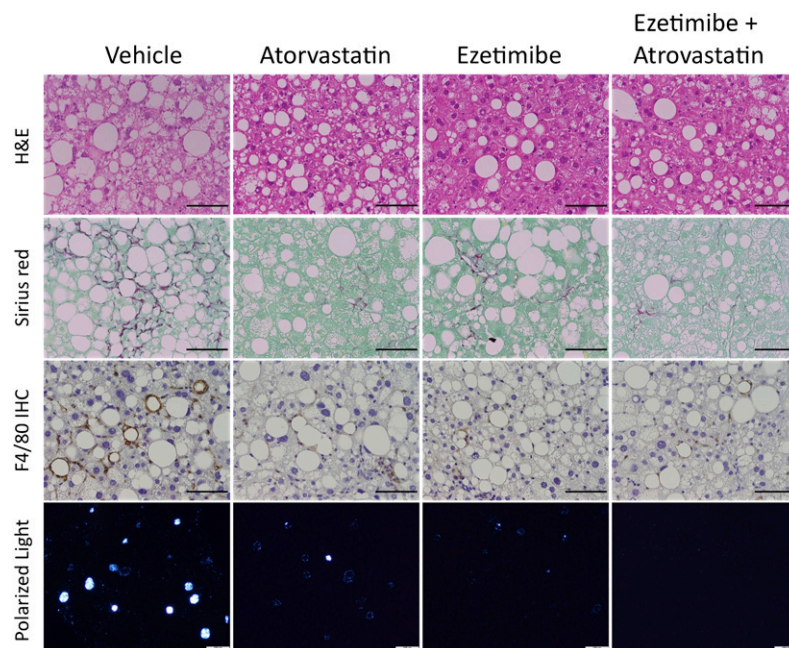


Fig. 1. Treatment with ezetimibe and atorvastatin eliminates hepatic cholesterol crystals and ameliorates inflammation and fibrosis. Liver sections of *foz/foz* mice on an atherogenic diet treated with “vehicle” (control), ezetimibe, or atorvastatin or with a combination of both ezetimibe and atorvastatin (“combination”) and stained with hematoxylin and eosin (H&E), Sirius red (for collagen), anti-F4/80 antibodies (for macrophages), or unstained frozen sections viewed with polarized light for birefringent cholesterol crystals. H&E or Sirius red stained liver sections demonstrate that *foz/foz* mice on an atherogenic diet treated with “vehicle” (control) developed fibrosing NASH. In contrast, *foz/foz* mice treated with combination of ezetimibe and atorvastatin show resolution of fibrotic NASH. Anti-F4/80 staining, which identifies macrophages, shows multiple rings of macrophages forming CLSs as they surround hepatocyte lipid droplets in the vehicle-treated mice. In the ezetimibe- and/or atorvastatin-treated mice, mostly scattered isolated macrophages were seen, with rare CLSs in the ezetimibe- or atorvastatin-treated mice and none in the mice treated with both drugs. Frozen liver sections viewed with polarized light demonstrate birefringence within a large proportion of lipid droplets in the “vehicle”-treated group (control), including droplets that are entirely birefringent appearing as a “Maltese cross.” There was progressively less birefringence in the atorvastatin-treated and ezetimibe-treated groups and almost no birefringence in the group that was treated with both drugs. This birefringence is due to cholesterol crystallization as demonstrated by filipin staining in Figure 3. Black scale bars are 50 μ m; white scale bars are 100 μ m. IHC, immunohistochemistry.

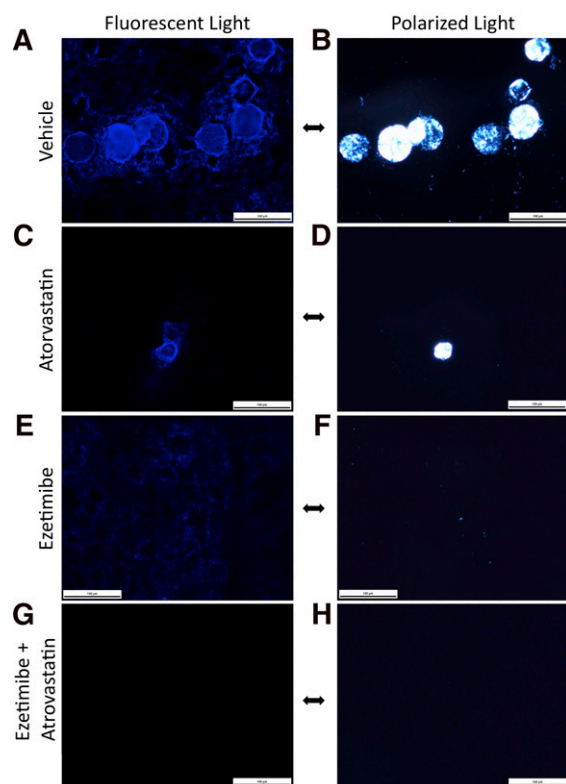


Fig. 2. Birefringent material within hepatocyte lipid droplets stains with filipin, demonstrating the presence of cholesterol crystals. Frozen liver sections from *foz/foz* mice fed a high-fat, high-cholesterol diet for 24 weeks, with the last 8 weeks supplemented with vehicle (A, B), ezetimibe (C, D), atorvastatin (E, F), or both ezetimibe and atorvastatin (G, H). The sections are stained with filipin (blue) to identify free cholesterol. Each section is viewed with polarized light (to demonstrate cholesterol crystals) or fluorescent light (to demonstrate filipin). Mice supplemented with vehicle, which developed NASH, had strongly birefringent crystals within a large proportion of lipid droplets (A) that also stain with filipin (B), demonstrating that they represent cholesterol crystals. Mice supplemented with both ezetimibe and atorvastatin, in which NASH was almost completely ameliorated, did not have any hepatic cholesterol crystals (G, H). Mice supplemented with only atorvastatin or only ezetimibe, in which NASH was only partly ameliorated, had some evidence of hepatic cholesterol crystals, especially in the atorvastatin group, but reduced as compared with the group that received both drugs.

treated with either ezetimibe or atorvastatin alone, partial (incomplete) resolution of CLSs was observed, with ezetimibe having a more profound effect than atorvastatin. There was striking correlation between the presence and density of cholesterol crystals and the presence/absence of CLSs. Cholesterol crystal presence and density also correlated with the presence/absence of histological NASH after treatment with vehicle versus atorvastatin and/or ezetimibe. These consistent relationships support a causal association between the formation of cholesterol crystals and CLSs in the pathogenesis of NASH.

Staining for neutrophils (antimyeloperoxidase) or T cells (anti-CD3) demonstrated that these cells were not associated with CLSs and were present in very low numbers relative to macrophages (data not shown).

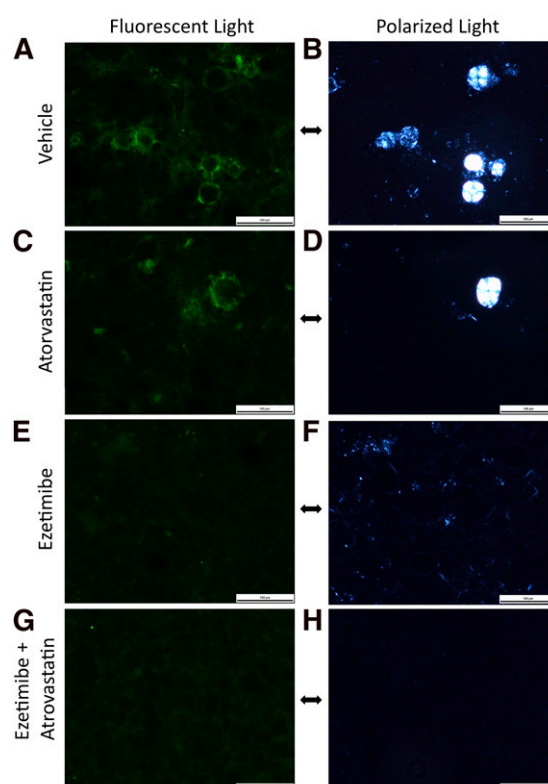


Fig. 3. KCs aggregate around hepatocytes that contain cholesterol crystals forming crown-like structures, which disperse after treatment with ezetimibe and atorvastatin. Frozen liver sections are shown from *foz/foz* mice fed a high-fat, high-cholesterol diet for 24 weeks, with the last 8 weeks supplemented with vehicle (A, B), ezetimibe (C, D), atorvastatin (E, F), or both ezetimibe and atorvastatin (G, H). The sections are stained with fluorescently labeled anti-TNF α antibodies (green) to identify activated KCs. Each section is viewed with either polarized light (to demonstrate cholesterol crystals) or fluorescent light (to demonstrate anti-TNF α). Mice supplemented with vehicle, which developed NASH, had strongly birefringent crystals within a large proportion of lipid droplets (A) that were surrounded by crown-like structures of activated macrophages (B). Mice supplemented with both ezetimibe and atorvastatin, in which NASH was almost completely ameliorated, did not have any hepatic cholesterol crystals (G) or macrophage crown-like structures (H). Mice supplemented with only atorvastatin or only ezetimibe, in which NASH was only partly ameliorated, had some evidence of hepatic cholesterol crystals and CLSs, especially in the atorvastatin group, but this amount was reduced as compared with the group that received both drugs.

Macrophages in CLSs surrounding steatotic hepatocytes with cholesterol crystals demonstrate NLRP3 activation

The KCs forming CLSs stained intensely positive for NLRP3 in vehicle-treated mice (Fig. 4A, B), whereas practically no NLRP3 staining was observed in mice treated with both ezetimibe and atorvastatin (Fig. 4C, D). Furthermore, the KCs in CLSs expressed activated (cleaved) caspase 1 in the vehicle-treated mice (Fig. 4E, F) but not in the ezetimibe- and atorvastatin-treated mice (Fig. 4G, H). The presence of cleaved caspase 1 confirms activation of the inflammasome pathway in KCs within CLS as a possible response to cholesterol crystals in NASH. mRNA gene expression levels of critical components of the NLRP3 inflammasome (*Nalp3*, *Asc*, and *Caspase1*) in whole liver

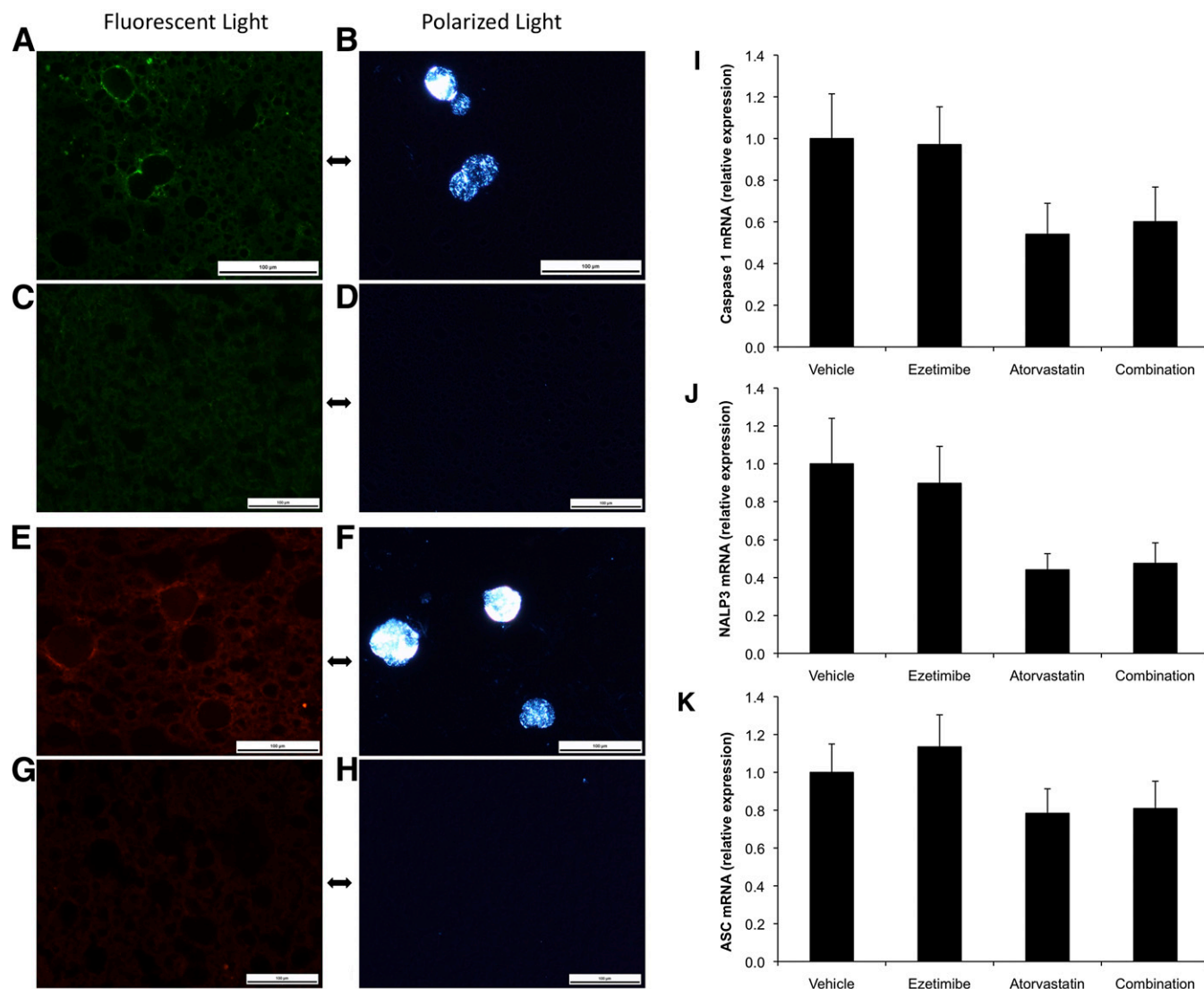


Fig. 4. KCs in CLS surrounding cholesterol crystal-containing remnant lipid droplets demonstrate activation of the NLRP3 inflammasome. Frozen liver sections are shown from *foz/foz* mice fed a high-fat, high-cholesterol diet for 24 weeks. Each section is viewed with polarized light (to demonstrate cholesterol crystals) or fluorescent light. **A and B:** KCs from vehicle-treated mice stained with anti-NLRP3 (identifies the NLRP3 inflammasome, colored green) showing that the macrophages that aggregate around heavily crystallized droplets forming CLSs exhibit critical components of the NLRP3 inflammasome. **C and D:** KCs from mice treated with both ezetimibe and atorvastatin stained with fluorescently labeled anti-NLRP3 and showing no staining. **E and F:** KCs from vehicle-treated mice stained with FLICA caspase 1, which identifies activated (cleaved) caspase 1 (red), showing that the macrophages in CLSs expressed activated caspase 1 and can potentially cleave pro-IL1 into IL1. **G and H:** KCs from mice treated with both ezetimibe and atorvastatin showing no staining. **I, J, and K:** mRNA expression levels (mean \pm SEM) for components of the NLRP3 inflammasome (*Caspase 1*, *Nalp3*, and *Asc*, respectively) demonstrating reduced expression in mice treated with ezetimibe and atorvastatin relative to vehicle-treated mice (this did not reach statistical significance defined as $P < 0.05$).

tissue was lower in ezetimibe- and atorvastatin-treated mice than in vehicle-treated mice, but this difference did not reach statistical significance (Fig. 4G–I).

DISCUSSION

We recently reported that cholesterol crystals were present in hepatocyte lipid droplets in the setting of experimental and human NASH but not in simple steatosis (18). CLSs of activated KCs surrounded and processed cholesterol crystal-containing remnant lipid droplets of dead

hepatocytes. Here we demonstrate that hepatic cholesterol crystals and CLSs are also present in a different mouse model of NAFLD/NASH, the *foz/foz* mouse on an atherogenic diet. Furthermore, treatment with ezetimibe and atorvastatin, which causes resolution of fibrotic NASH in these mice, also resulted in resolution of hepatic cholesterol crystals and CLSs. This suggests a causative association between hepatic cholesterol crystals and CLSs and the development of NASH. Because ezetimibe and atorvastatin are widely clinically available, our results could also inform future human clinical trials if hepatic cholesterol crystallization and formation of CLSs is further confirmed

to be an important pathogenetic mechanism in human NASH. Finally, our results suggest that hepatic cholesterol crystals mediate progression to NASH via activation of the NLRP3 inflammasome within the KCs that are exposed to cholesterol crystals in CLSs.

High levels of intracellular-free cholesterol can lead to cholesterol crystallization, which has been shown to result in cell toxicity in macrophages in the setting of atherosclerosis, potentially by physically disrupting the integrity of intracellular structures (27). Crystallized cholesterol originating in foamy macrophages is in fact an important contributor to the atheromatous plaque. By analogy with these mechanisms of cholesterol crystal formation and cellular toxicity in the setting of atherosclerosis, it is tempting to postulate that cholesterol crystallization within hepatocyte lipid droplets may also lead to cell toxicity. Dead hepatocytes containing cholesterol crystals within their remnant lipid droplets stimulate the aggregation of KCs around them, causing formation of the characteristic CLSs that we describe. Processing of the remnant lipid droplets by KCs creates even more free cholesterol as the cholesterol esters within the lipid droplets are hydrolyzed. This additional free cholesterol also crystallizes, leading to the intensely birefringent lipid droplets in the center of CLSs, some appearing as a “Maltese cross,” which represents supersaturated, metastable cholesterol in liquid crystalline form that is on the verge of undergoing a phase transition to cholesterol microcrystals. Further experiments are needed to specifically determine the factors that influence cholesterol crystallization within hepatocyte lipid droplets and how such cholesterol crystallization might affect the structure and function of the lipid droplet and induce cell toxicity or cell death.

Inflammasomes are molecular platforms activated upon cellular infection or stress that trigger the maturation of proinflammatory cytokines such as IL-1 β to engage innate immune defenses (28). The inflammasomes sense pathogen-associated molecular patterns in the cytosol as well as host-derived signals, known as “damage-associated molecular patterns,” which indicate cellular damage or stress. The NLRP3 inflammasome also drives inflammation in response to exposure to crystals that are known to cause human chronic inflammatory conditions (29–32). Cholesterol crystals are the latest addition to the types of crystals shown to activate the NLRP3 inflammasome in the setting of an important, human chronic inflammatory condition, in this case atherosclerosis (21, 22). We demonstrated that KCs become exposed to crystallized cholesterol as they aggregate into CLSs around remnant lipid droplets containing cholesterol crystals (Fig. 3). We also showed that KCs in CLSs stain strongly positive with NLRP3. Taken together with the recent literature on NLRP3 activation in macrophages by cholesterol crystals in atherosclerosis, our findings suggest that exposure of KCs to cholesterol crystals may activate the NLRP3 inflammasome, leading to chronic inflammation and contributing to the development of NASH. Specifically designed experiments are needed to prove whether the NLRP3 inflammasome is an important mediator of chronic


inflammation induced by exposure of hepatocytes and KCs to cholesterol crystals.

There was a striking correlation between the presence/absence of hepatic cholesterol crystals and CLSs and the presence/absence of NASH after treatment with ezetimibe and atorvastatin. The *foz/foz* mice that were treated with ezetimibe and atorvastatin for the last 8 weeks of the experiment had almost complete resolution of cholesterol crystals (0.01% of liver surface area as compared with 3.3% in the vehicle-treated mice) and CLSs, as shown in Figs. 2 and 3, together with a profound amelioration of fibrotic NASH. Ezetimibe alone and atorvastatin alone had intermediate effects on cholesterol crystallization and formation of CLSs, with the effect of ezetimibe being greater than that of atorvastatin, again correlating with the degree of resolution of fibrotic NASH. These tight correlations point to a causative association between hepatic cholesterol crystals, CLSs, and NASH.

The additive effects of ezetimibe and atorvastatin on ameliorating hepatic cholesterol crystals can be explained by the fact that they reduce the exposure of the liver to cholesterol via different and independent pathways. Atorvastatin inhibits hepatic cholesterol synthesis by inhibiting HMG-CoA reductase, whereas ezetimibe inhibits the intestinal absorption of cholesterol by binding Niemann-Pick C1 like-1 (33). In addition, because Niemann-Pick C1 like-1 is expressed in hepatocytes and biliary epithelial cells as well as in enterocytes (34), ezetimibe may interrupt the hepatic recycling of cholesterol secreted into bile and taken up by biliary duct epithelium. Our results do not suggest that the mechanism by which hepatic cholesterol exposure is reduced is important; rather, the degree of reduction of hepatic cholesterol exposure seems to be more important than the mechanism by which it is achieved.

An emerging literature suggests that cholesterol-lowering drugs may be beneficial for hepatic outcomes in human NASH. Four randomized control trials (35–38) (a total of 719 participants) assessed statins in patients with NAFLD. Statins improved alanine aminotransferase and radiological steatosis in hyperlipidemic patients with NAFLD and caused dramatic reductions in cardiovascular events (35). Only one study evaluated histological outcomes and found no improvement in hepatic inflammation or fibrosis after 12 months of simvastatin; however, only 10 patients underwent repeat liver biopsies, and the study was clearly underpowered (38). In small pilot clinical trials, treatment of patients with biopsy-proven NASH with ezetimibe for 6 (16) or 24 (17) months was associated with improvements in hepatic steatosis, inflammation, and hepatocyte ballooning but not fibrosis (17). However, these studies were not randomized or controlled. In a small, randomized controlled trial, addition of ezetimibe to a moderate weight loss diet for 16 weeks in obese subjects significantly improved hepatic steatosis, inflammation, and LDL-apoB-100 metabolism (39). Finally, in a recent small, open-label randomized control trial, treatment with ezetimibe for 6 months improved hepatic fibrosis but increased hemoglobin A1c levels (40). In summary, although existing data showing that cholesterol-lowering drugs benefit

NAFLD pathology and disease progression are fragmentary, this approach is worthy of controlled study, particularly using aggressive cholesterol-lowering approaches now recommended for those at high risk of cardiovascular events (41).

Further work is required in humans to establish more firmly that hepatic cholesterol crystals and CLSs are associated with NASH but not with simple steatosis. Our current work in mice might be relevant because ezetimibe and atorvastatin are clinically available and could be used in preliminary clinical trials to determine if they lead to resolution of hepatic cholesterol crystals and CLSs. Finally, the mechanistic importance of cholesterol crystal-mediated activation of NLRP3 inflammasomes in KCs in NASH requires further elucidation because this could provide a novel, much-needed therapeutic pathway for this common liver disease. 

REFERENCES

- Matteoni, C. A., Z. M. Younossi, T. Gramlich, N. Boparai, Y. C. Liu, and A. J. McCullough. 1999. Nonalcoholic fatty liver disease: a spectrum of clinical and pathological severity. *Gastroenterology*. **116**: 1413–1419.
- Bugianesi, E., N. Leone, E. Vanni, G. Marchesini, F. Brunello, P. Carucci, A. Musso, P. De Paolis, L. Capussotti, M. Salizzoni, et al. 2002. Expanding the natural history of nonalcoholic steatohepatitis: from cryptogenic cirrhosis to hepatocellular carcinoma. *Gastroenterology*. **123**: 134–140.
- Puri, P., R. A. Baillie, M. M. Wiest, F. Mirshahi, J. Choudhury, O. Cheung, C. Sargeant, M. J. Contos, and A. J. Sanyal. 2007. A lipidomic analysis of nonalcoholic fatty liver disease. *Hepatology*. **46**: 1081–1090.
- Matsuzawa, N., T. Takamura, S. Kurita, H. Misu, T. Ota, H. Ando, M. Yokoyama, M. Honda, Y. Zen, Y. Nakanuma, et al. 2007. Lipid-induced oxidative stress causes steatohepatitis in mice fed an atherogenic diet. *Hepatology*. **46**: 1392–1403.
- Zheng, S., L. Hoos, J. Cook, G. Tetzloff, H. Davis, Jr., M. van Heek, and J. J. Hwa. 2008. Ezetimibe improves high fat and cholesterol diet-induced non-alcoholic fatty liver disease in mice. *Eur. J. Pharmacol.* **584**: 118–124.
- Van Rooyen, D. M., C. Z. Larter, W. G. Haigh, M. M. Yeh, G. Ioannou, R. Kuver, S. P. Lee, N. C. Teoh, and G. C. Farrell. 2011. Hepatic free cholesterol accumulates in obese, diabetic mice and causes nonalcoholic steatohepatitis. *Gastroenterology* **141**: 1393–1403, 1403.e1–5.
- Savard, C., E. V. Tartaglione, R. Kuver, W. G. Haigh, G. C. Farrell, S. Subramanian, A. Chait, M. M. Yeh, L. S. Quinn, and G. N. Ioannou. 2013. Synergistic interaction of dietary cholesterol and dietary fat in inducing experimental steatohepatitis. *Hepatology*. **57**: 81–92.
- Van Rooyen, D. M., L. T. Gan, M. M. Yeh, W. G. Haigh, C. Z. Larter, G. Ioannou, N. C. Teoh, and G. C. Farrell. 2013. Pharmacological cholesterol lowering reverses fibrotic NASH in obese, diabetic mice with metabolic syndrome. *J. Hepatol.* **59**: 144–152.
- Wouters, K., M. van Bilsen, P. J. van Gorp, V. Bieghs, D. Lutjohann, A. Kerksiek, B. Staels, M. H. Hofker, and R. Shiri-Sverdlov. 2010. Intrahepatic cholesterol influences progression, inhibition and reversal of non-alcoholic steatohepatitis in hyperlipidemic mice. *FEBS Lett.* **584**: 1001–1005.
- Wouters, K., P. J. van Gorp, V. Bieghs, M. J. Gijbels, H. Duimel, D. Lutjohann, A. Kerksiek, R. van Kruchten, N. Maeda, B. Staels, et al. 2008. Dietary cholesterol, rather than liver steatosis, leads to hepatic inflammation in hyperlipidemic mouse models of nonalcoholic steatohepatitis. *Hepatology*. **48**: 474–486.
- Bieghs, V., P. J. Van Gorp, K. Wouters, T. Hendriks, M. J. Gijbels, M. van Bilsen, J. Bakker, C. J. Binder, D. Lutjohann, B. Staels, et al. 2012. LDL receptor knock-out mice are a physiological model particularly vulnerable to study the onset of inflammation in non-alcoholic fatty liver disease. *PLoS ONE*. **7**: e30668.
- Subramanian, S., L. Goodspeed, S. Wang, J. Kim, L. Zeng, G. N. Ioannou, W. G. Haigh, M. M. Yeh, K. V. Kowdley, K. D. O'Brien, et al. 2011. Dietary cholesterol exacerbates hepatic steatosis and inflammation in obese LDL receptor-deficient mice. *J. Lipid Res.* **52**: 1626–1635.
- Itoh, M., T. Suganami, N. Nakagawa, M. Tanaka, Y. Yamamoto, Y. Kamei, S. Terai, I. Sakaida, and Y. Ogawa. 2011. Melanocortin 4 receptor-deficient mice as a novel mouse model of nonalcoholic steatohepatitis. *Am. J. Pathol.* **179**: 2454–2463.
- Chan, J., F. E. Sharkey, R. S. Kushwaha, J. F. VandeBerg, and J. L. VandeBerg. 2012. Steatohepatitis in laboratory opossums exhibiting a high lipemic response to dietary cholesterol and fat. *Am. J. Physiol. Gastrointest. Liver Physiol.* **303**: G12–G19.
- Ioannou, G. N., O. B. Morrow, M. L. Connole, and S. P. Lee. 2009. Association between dietary nutrient composition and the incidence of cirrhosis or liver cancer in the United States population. *Hepatology*. **50**: 175–184.
- Yoneda, M., K. Fujita, Y. Nozaki, H. Endo, H. Takahashi, K. Hosono, K. Suzuki, H. Mawatari, H. Kirikoshi, M. Inamori, et al. 2010. Efficacy of ezetimibe for the treatment of non-alcoholic steatohepatitis: An open-label, pilot study. *Hepatol. Res.* **40**: 566–573.
- Park, H., T. Shima, K. Yamaguchi, H. Mitsuyoshi, M. Minami, K. Yasui, Y. Itoh, T. Yoshikawa, M. Fukui, G. Hasegawa, et al. 2011. Efficacy of long-term ezetimibe therapy in patients with nonalcoholic fatty liver disease. *J. Gastroenterol.* **46**: 101–107.
- Ioannou, G. N., W. G. Haigh, D. Thorning, and C. Savard. 2013. Hepatic cholesterol crystals and crown-like structures distinguish NASH from simple steatosis. *J. Lipid Res.* **54**: 1326–1334.
- Cinti, S., G. Mitchell, G. Barbatelli, I. Murano, E. Ceresi, E. Faloia, S. Wang, M. Fortier, A. S. Greenberg, and M. S. Obin. 2005. Adipocyte death defines macrophage localization and function in adipose tissue of obese mice and humans. *J. Lipid Res.* **46**: 2347–2355.
- Strissel, K. J., Z. Stancheva, H. Miyoshi, J. W. Perfield 2nd, J. DeFuria, Z. Jick, A. S. Greenberg, and M. S. Obin. 2007. Adipocyte death, adipose tissue remodeling, and obesity complications. *Diabetes*. **56**: 2910–2918.
- Duewell, P., H. Kono, K. J. Rayner, C. M. Sirois, G. Vladimer, F. G. Bauernfeind, G. S. Abela, L. Franchi, G. Nunez, M. Schnurr, et al. 2010. NLRP3 inflammasomes are required for atherogenesis and activated by cholesterol crystals. *Nature*. **464**: 1357–1361.
- Rajamaki, K., J. Lappalainen, K. Oorni, E. Valimaki, S. Matikainen, P. T. Kovanen, and K. K. Eklund. 2010. Cholesterol crystals activate the NLRP3 inflammasome in human macrophages: a novel link between cholesterol metabolism and inflammation. *PLoS ONE*. **5**: e11765.
- Heydet, D., L. X. Chen, C. Z. Larter, C. Inglis, M. A. Silverman, G. C. Farrell, and M. R. Leroux. 2013. A truncating mutation of *Alms1* reduces the number of hypothalamic neuronal cilia in obese mice. *Dev. Neurobiol.* **73**: 1–13.
- Kleiner, D. E., E. M. Brunt, M. Van Natta, C. Behling, M. J. Contos, O. W. Cummings, L. D. Ferrell, Y. C. Liu, M. S. Torbenson, A. Unalp-Arida, et al. 2005. Design and validation of a histological scoring system for nonalcoholic fatty liver disease. *Hepatology*. **41**: 1313–1321.
- Rudolf, M., and C. A. Curcio. 2009. Esterified cholesterol is highly localized to Bruch's membrane, as revealed by lipid histochemistry in whole mounts of human choroid. *J. Histochem. Cytochem.* **57**: 731–739.
- Ganz, M., T. Csak, B. Nath, and G. Szabo. 2011. Lipopolysaccharide induces and activates the Nalp3 inflammasome in the liver. *World J. Gastroenterol.* **17**: 4772–4778.
- Tabas, I. 2002. Consequences of cellular cholesterol accumulation: basic concepts and physiological implications. *J. Clin. Invest.* **110**: 905–911.
- Schroder, K., and J. Tschopp. 2010. The inflammasomes. *Cell*. **140**: 821–832.
- Martinon, F., V. Petrilli, A. Mayor, A. Tardivel, and J. Tschopp. 2006. Gout-associated uric acid crystals activate the NALP3 inflammasome. *Nature*. **440**: 237–241.
- Hornung, V., F. Bauernfeind, A. Halle, E. O. Samstad, H. Kono, K. L. Rock, K. A. Fitzgerald, and E. Latz. 2008. Silica crystals and aluminum salts activate the NALP3 inflammasome through phagosomal destabilization. *Nat. Immunol.* **9**: 847–856.
- Dostert, C., V. Petrilli, R. Van Bruggen, C. Steele, B. T. Mossman, and J. Tschopp. 2008. Innate immune activation through Nalp3 inflammasome sensing of asbestos and silica. *Science*. **320**: 674–677.
- Cassel, S. L., S. C. Eisenbarth, S. S. Iyer, J. J. Sadler, O. R. Colegio, L. A. Tephly, A. B. Carter, P. B. Rothman, R. A. Flavell, and F. S. Sutterwala. 2008. The Nalp3 inflammasome is essential for the development of silicosis. *Proc. Natl. Acad. Sci. USA*. **105**: 9035–9040.

33. Hawes, B. E., K. A. O'Neill, X. Yao, J. H. Crona, H. R. Davis, Jr., M. P. Graziano, and S. W. Altmann. 2007. In vivo responsiveness to ezetimibe correlates with niemann-pick C1 like-1 (NPC1L1) binding affinity: Comparison of multiple species NPC1L1 orthologs. *Mol. Pharmacol.* **71**: 19–29.
34. Betters, J. L., and L. Yu. 2010. NPC1L1 and cholesterol transport. *FEBS Lett.* **584**: 2740–2747.
35. Athyros, V. G., K. Tziomalos, T. D. Gossios, T. Griva, P. Anagnostis, K. Kargiotis, E. D. Pagourelis, E. Theocharidou, A. Karagiannis, D. P. Mikhailidis, et al. 2010. Safety and efficacy of long-term statin treatment for cardiovascular events in patients with coronary heart disease and abnormal liver tests in the Greek Atorvastatin and Coronary Heart Disease Evaluation (GREACE) Study: a post-hoc analysis. *Lancet.* **376**: 1916–1922.
36. Athyros, V. G., D. P. Mikhailidis, T. P. Didangelos, O. I. Giouleme, E. N. Liberopoulos, A. Karagiannis, A. I. Kakafika, K. Tziomalos, A. K. Burroughs, and M. S. Elisaf. 2006. Effect of multifactorial treatment on non-alcoholic fatty liver disease in metabolic syndrome: a randomised study. *Curr. Med. Res. Opin.* **22**: 873–883.
37. Foster, T., M. J. Budoff, S. Saab, N. Ahmadi, C. Gordon, and A. D. Guerci. 2011. Atorvastatin and antioxidants for the treatment of nonalcoholic fatty liver disease: the St Francis Heart Study randomized clinical trial. *Am. J. Gastroenterol.* **106**: 71–77.
38. Nelson, A., D. M. Torres, A. E. Morgan, C. Fincke, and S. A. Harrison. 2009. A pilot study using simvastatin in the treatment of nonalcoholic steatohepatitis: a randomized placebo-controlled trial. *J. Clin. Gastroenterol.* **43**: 990–994.
39. Chan, D. C., G. F. Watts, S. K. Gan, E. M. Ooi, and P. H. Barrett. 2010. Effect of ezetimibe on hepatic fat, inflammatory markers, and apolipoprotein B-100 kinetics in insulin-resistant obese subjects on a weight loss diet. *Diabetes Care.* **33**: 1134–1139.
40. Takeshita, Y., T. Takamura, M. Honda, Y. Kita, Y. Zen, K. Kato, H. Misu, T. Ota, M. Nakamura, K. Yamada, et al. 2014. The effects of ezetimibe on non-alcoholic fatty liver disease and glucose metabolism: a randomised controlled trial. *Diabetologia.* **57**: 878–890.
41. Smith, S. C., Jr., and S. M. Grundy. 2014. 2013 ACC/AHA guideline recommends fixed-dose strategies instead of targeted goals to lower blood cholesterol. *J. Am. Coll. Cardiol.* **64**: 601–612.